Journal of Materials Chemistry C

RSC Publishing

PAPER

View Article Online
View Journal

Cite this: DOI: 10.1039/c3tc30536h

Star-shaped molecules containing both azo chromophores and carbazole units as a new type of photoresponsive amorphous material

Jianjun Yin, Gang Ye and Xiaogong Wang*

Received 21st March 2013
Accepted 17th April 2013

DOI: 10.1039/c3tc30536h

www.rsc.org/MaterialsC

We synthesized a series of star-shaped molecules containing both azo chromophores and carbazole units (*n*Cz-AZ-X), where *n* is the number of carbazole units ($n = 3$ and 6) and X represents cyano (CN) and nitro (NT) as the electron-withdrawing groups on the azobenzenes. The azo compounds existed as amorphous solids at room temperature with glass transition temperatures (T_g) of 89, 86, 74 and 73 °C for **3Cz-AZ-CN**, **3CZ-AZ-NT**, **6Cz-AZ-CN** and **6Cz-AZ-NT**, respectively. Thin solid films of the azo molecular glasses were obtained by spin-coating. The formation of the photoinduced self-structured surface patterns was investigated by irradiating the solid thin films of the azo molecular glasses with a uniform laser beam (532 nm, 200 mW cm^{-2}) at normal incidence. The formation of surface-relief-gratings (SRGs) was studied by exposing the thin films to an interference pattern of the laser beams (532 nm, 80 mW cm^{-2}). The formation of both the self-structured surface patterns and SRGs showed a close correlation with the electron-withdrawing groups of the azo chromophores and the content of the carbazole units in the molecules. The development of these new star-shaped molecules can add a new member to the category of azo molecular glasses and lead to a deeper understanding of the photoinduced effects and their correlation with molecular structures.

1 Introduction

In the past decades, azo polymers (polymers containing aromatic azo chromophores) have attracted considerable attention for their interesting properties and various applications.[1–8] When irradiated with light at appropriate wavelengths, the azobenzene moieties in the polymers undergo reversible *trans–cis* isomerization, which triggers a variety of photoresponsive variations.[4–8] Photoinduced surface pattern formation includes some of the most interesting properties of azo polymers.[9,10] Surface-relief-grating (SRG) formation refers to the reversible surface modulation on azo polymer films when irradiated with interfering laser beams.[5–7,9,10] Sinusoidal surface patterns with modulated depth on the submicrometer scale can be inscribed on azo polymer films at a temperature well below the glass transition temperatures (T_gs) of the polymers and erased by heating the samples to a temperature above their T_gs.[6,9,10] Photoinduced SRG formation has been intensively studied for its potential application in areas such as information storage, diffractive optical elements, sensors and actuators.[5–8] Although it has been actively studied in recent years, the mechanism of SRG formation still remains a puzzling issue requiring further elucidation.[11–16] Self-structured surface pattern formation is another type of light-induced surface modulation.[17] It is characterized by the spontaneous formation of submicrometer hexagonal patterns on the azo polymer films after irradiation with a uniform single laser beam at normal incidence. The patterns comprise regularly spaced pillar-like structures with a saturated height of about 100 nm.[17,18] Compared with the extensive exploration of the SRGs, the research effort devoted to the photoinduced self-structured surface pattern formation is rather limited and even less is known about its formation mechanism.

Amorphous molecular materials, also known as "molecular glasses", are low molecular-weight organic compounds that exist as stable amorphous materials near and above room temperature.[19,20] By vapor deposition or spin-coating, transparent amorphous solid films of these materials can be prepared. In recent years, incorporating azo chromophores into the amorphous molecular materials has offered a promising new possibility for developing photoresponsive materials.[21–23] Compared with azo polymers, the amorphous molecular materials containing azo chromophores (azo molecular glasses) can show several attractive characteristics such as high chromophore density and absence of chain entanglement.[19b] Moreover, the well-defined structures of azo molecular glasses enable them to be an ideal candidate for mechanism study. Several types of azo molecular glasses have been developed through different molecular design motifs and synthetic methods.[19–30] SRGs can be inscribed on an azo molecular glass film with a fast

Department of Chemical Engineering, Key Laboratory of Advanced Materials (MOE), Tsinghua University, Beijing 100084, P. R. China. E-mail: wxg-dce@mail.tsinghua.edu.cn; Fax: +86 10 6278 1003; Tel: +86 10 6279 6171

growth rate and large surface modulation.[26–30] However, as a new class of potential photo- and electro-active organic materials, only limited types of the azo molecular glasses have been developed.

According to the strategy for molecular design, the amorphous molecular materials should incorporate rigid moieties to maintain the amorphous state at room temperature.[19,20] Typically, biphenyl and biphenylene units have been widely used as building blocks to construct molecular glasses. For most reported azo molecular glasses, the biphenyl or biphenylene units and azobenzene are tightly anchored by rigid tris(phenyl) cores.[19–25] At the current stage, new building blocks are still needed to further develop azo molecular glasses. Carbazoles have been widely investigated as building blocks to prepare photoconductive polymers, non-linear optical polymers, and organic/polymeric materials for plastic electronics and photovoltaics.[31–33] Introducing carbazole moieties into azo molecular glasses can be an attractive strategy to develop new types of photoresponsive materials. These materials can show a sensitive response to light irradiation to form SRGs, self-structured surface patterns and exhibit other new functions. However, to our knowledge, a molecular glass containing both azo chromophore and carbazole group in the molecular structure has not been reported in the literature yet.

In this study, we have developed a new molecular design strategy to synthesize star-shaped azo molecules to contain both azo chromophores and carbazole groups as amorphous materials. The molecules were constructed by connecting three azo chromophores to a cyanuric acid core and carbazole moieties were introduced into the molecules through flexible spacers. Transparent solid films could be obtained by spin-coating with solutions of these azo compounds. The structure and property relationship of the azo molecular glasses, in particular for surface modulation in response to light irradiation, was investigated in detail.

2 Experimental

2.1 Materials and synthesis

Tetrahydrofuran (THF) was first refluxed with cuprous chloride for 1 h and distilled; then refluxed with sodium for 6 h and distilled before use. *N*,*N*-Dimethylformamide (DMF) was azeotropically distilled with benzene six times for dehydration and then purified by vacuum distillation. Dichloromethane (DCM) was washed with 98% H_2SO_4 and distilled. All other chemicals and solvents were commercially purchased and used as received without further purification.

6-(*H*-Carbazol-9-yl)hexanoic acid. Carbazole (3.34 g, 20 mmol) was added to a mixture of potassium hydroxide powder (4 g) and anhydrous DMF (50 mL), which was magnetically stirred at room temperature for 1 h. 6-Bromohexanoic acid (4.88 g, 25 mmol) was slowly added into the reaction mixture. The mixture was stirred at room temperature for 3 h and then poured into plenty of water. The insoluble solid was removed from the aqueous solution by filtration. The clear solution was then adjusted to neutral pH. The precipitate formed in the solution was collected by filtration and washed with plenty of water. The final product was vacuum dried at 70 °C for 24 h. Yield: 75%. ^{1}H NMR (DMSO-d_6) δ (ppm): 1.32 (m, 2H), 1.52 (m, 2H), 1.77 (m, 2H), 2.14 (t, 2H), 4.38 (t, 2H), 7.19 (t, 2H), 7.44 (t, 2H), 7.59 (d, 2H), 8.14 (d, 2H), 11.99 (br, 1H).

2-(Phenylamino)ethanol. A mixture of aniline (9.30 g, 0.1 mol), 2-chloroethanol (8.05 g, 0.1 mol), anhydrous K_2CO_3 (13 g, 0.1 mmol) and KI (1 g) was heated to 80 °C under nitrogen protection with vigorous stirring for 12 h. The residue was diluted with ethyl acetate. The solution was filtered and the solvent was then removed by evaporation in a vacuum. The crude product was further purified by column chromatography (ethyl acetate–hexane, $v_1/v_2 = 1:2$). Yield: 41%. ^{1}H NMR ($CDCl_3$-d) δ (ppm): 3.32 (t, 2H), 3.80 (t, 2H), 6.65 (d, 2H), 6.73 (t, 1H), 7.18 (t, 2H).

1,3,5-Tris(2-hydroxy-3-(methyl(phenyl)amino)propyl)-1,3,5-triazinane-2,4,6-trione (Tr-AN). Tr-AN was obtained from the reaction between 1,3,5-tris(oxiran-2-yl-methyl)-1,3,5-triazinane-2,4,6-trione and *N*-methylaniline according to the literature.[30] Yield: 85%. ^{1}H NMR (DMSO-d_6) δ (ppm): 2.92 (s, 9H), 3.20 (m, 3H), 3.45 (m, 3H), 3.68 (m, 3H), 3.90 (m, 3H), 4.07 (m, 3H), 4.91 (d, 3H), 6.57 (t, 3H), 6.66 (d, 6H), 7.12 (t, 6H).

1,3,5-Tris(2-hydroxy-3-((2-hydroxyethyl)(phenyl)amino)propyl)-1,3,5-triazinane-2,4,6-trione (6-Tr-AN). This compound was synthesized *via* a procedure similar to that described above for **Tr-AN** preparation by using *N*-(2-hydroxyethyl)aniline instead of *N*-methylaniline in the reaction. Yield: 75%. ^{1}H NMR (DMSO-d_6) δ (ppm): 3.22 (m, 3H), 3.40 (m, 3H), 3.48–3.60 (m, 12H), 3.71 (m, 3H), 3.91 (m, 3H), 4.09 (m, 3H), 4.71 (br, 3H), 5.06 (br, 3H), 6.54 (t, 3H), 6.66 (d, 6H), 7.10 (t, 6H).

3Cz-AN. 3Cz-AN was synthesized by esterification reaction between **Tr-AN** and 6-(*H*-carbazol-9-yl)hexanoic acid. Dicyclohexylcarbodiimide (DCC, 1.03 g, 5 mmol) was added to a magnetically stirred dichloromethane solution (30 mL) of 4-dimethylaminopyridine (DMAP, catalytic amount), 6-(*H*-carbazol-9-yl)hexanoic acid (1.40 g, 5 mmol) and **Tr-AN** (0.93 g, 1.5 mmol) at 0 °C. After the solution was stirred at room temperature for 12 h, it was filtered and the solvent was removed by evaporation in a vacuum. The crude product was further purified by column chromatography (CH_2Cl_2, the first component). Yield: 85%. ^{1}H NMR (DMSO-d_6), 80 °C, δ (ppm): 1.10 (6H), 1.29 (6H), 1.59 (6H), 1.90–1.94 (6H), 2.72 (9H), 3.41 (3H), 3.82 (3H), 4.05 (3H), 4.19 (6H), 5.25 (3H), 6.51 (3H), 6.62 (6H), 7.02 (6H), 7.14 (6H), 7.38 (6H), 7.42 (6H), 8.08 (6H).

6Cz-AN. This compound was synthesized *via* a procedure similar to that described above for **3Cz-AN** preparation by using **6-Tr-AN** instead of **Tr-AN** in the reaction. Yield: 83%. ^{1}H NMR (DMSO-d_6), 80 °C, δ (ppm): 1.06–1.67 (36H), 1.92–2.07 (12H), 3.34–3.44 (12H), 3.81 (3H), 4.00 (6H), 4.10 (3H), 4.13 (6H), 4.26 (6H), 5.23 (3H), 6.48 (3H), 6.66 (6H), 7.00 (6H), 7.12 (12H), 7.37–7.45 (24H), 8.06 (12H).

3Cz-AZ-CN. 4-Aminobenzontrile (0.30 g, 2.5 mmol) was mixed with sulfuric acid (0.5 mL) and glacial acetic acid (7 mL). The diazonium salt was prepared by slowly adding an aqueous solution of sodium nitrite (0.2 g, 2.9 mmol in 1 mL of water) into the 4-aminobenzontrile solution. The mixture was stirred at 5 °C for 5 min and then added dropwise into a solution of **3Cz-AN** (0.70 g, 0.5 mmol) in DMF (50 mL). The solution was stirred

at 0 °C for 12 h and then poured into plenty of water. The precipitate collected by filtration was then dissolved in THF and precipitated again with petroleum ether. The final product was vacuum dried at 70 °C for 24 h. Yield: 87%. DSC: T_g 89 °C. M_w/M_n (GPC): 1.06. IR (KBr, cm^{-1}): 3051 (carbazole), 2935, 2846 ($-CH_2$), 2225 (C≡N), 1736, 1697 (C=O), 1597, 1516, 1462 (Benz ring, carbazole). ^{1}H NMR (DMSO-d_6), 80 °C, δ (ppm): 1.05 (6H), 1.25 (6H), 1.52 (6H), 1.93 (6H), 2.90 (9H), 3.63–3.68 (6H), 3.92 (3H), 4.11 (9H), 5.33 (3H), 6.78 (6H), 7.11 (6H), 7.32 (12H), 7.70 (12H), 7.80 (6H), 8.05 (6H).

3Cz-AZ-NT. This compound was synthesized by the azo-coupling reaction between **3Cz-AN** and the diazonium salt of 4-nitroaniline *via* a similar method used for preparing **3Cz-AZ-CN**. Yield: 80%. DSC: T_g 86 °C. M_w/M_n (GPC): 1.04. IR (KBr, cm^{-1}): 3050 (carbazole), 2933, 2862 ($-CH_2$), 1736, 1697 (C=O), 1601, 1518, 1454 (Benz ring, carbazole), 1340 ($-NO_2$). ^{1}H NMR (DMSO-d_6), 80 °C, δ (ppm): 1.07–1.15 (6H), 1.28–1.32 (6H), 1.54–1.59 (6H), 1.90–1.98 (6H), 2.84–2.89 (9H), 3.48–3.71 (6H), 3.92 (3H), 4.12 (9H), 5.31 (3H), 6.79 (6H), 7.10 (6H), 7.32 (12H), 7.72–7.80 (12H), 8.03 (6H), 8.19–8.25 (6H).

6Cz-AZ-CN. This compound was synthesized *via* a procedure similar to that described above for **3Cz-AZ-CN** preparation by using **6Cz-AN** instead of **3Cz-AN** in the reaction. Yield: 79%. DSC: T_g 74 °C. M_w/M_n (GPC): 1.05. IR (KBr, cm^{-1}): 3049 (carbazole), 2933, 2862 ($-CH_2$), 2224 (C≡N), 1734, 1697 (C=O), 1597, 1512, 1452 (Benz ring, carbazole). ^{1}H NMR (DMSO-d_6), 80 °C, δ (ppm): 1.01–1.65 (36H), 1.96–2.08 (12H), 3.53–3.66 (12H), 3.91 (3H), 4.04–4.07 (12H), 4.17 (3H), 4.22 (6H), 5.31 (3H), 6.84 (6H), 7.12 (12H), 7.28 (12H), 7.35–7.42 (12H), 7.66 (12H), 7.75 (6H), 8.06 (12H).

6Cz-AZ-NT. This compound was synthesized *via* a procedure similar to that described above for **3Cz-AZ-NT** preparation by using **6Cz-AN** instead of **3Cz-AN** in the reaction. Yield: 86%. DSC: T_g 73 °C. M_w/M_n (GPC): 1.05. IR (KBr, cm^{-1}): 3049 (carbazole), 2933, 2860 ($-CH_2$), 1736, 1697 (C=O), 1599, 1514, 1452 (Benz ring, carbazole), 1338 ($-NO_2$). ^{1}H NMR (DMSO-d_6), 80 °C, δ (ppm): 1.04–1.67 (36H), 1.99–2.10 (12H), 3.57–3.69 (12H), 3.95 (3H), 3.97–4.10 (12H), 4.23 (9H), 5.38 (3H), 6.87 (6H), 7.11 (12H), 7.29 (12H), 7.36–7.44 (12H), 7.69 (12H), 8.02 (6H), 8.16 (12H).

2.2 Characterization

^{1}H NMR spectra were obtained on a JOEL JNM-ECA300 NMR spectrometer. IR spectra were determined using a Nicolet 560-IR FT-IR spectrophotometer by incorporating the powder samples in KBr disks. The UV-vis spectra of the samples were recorded using a Perkin-Elmer Lambda Bio-40 spectrophotometer. The molecular weights (MWs) and distributions were determined using a gel permeation chromatographic (GPC) apparatus, which was operated at 25 °C using THF as the eluent (1 mL min^{-1}). The instrument was equipped with a refractive index (RI) detector (Wyatt Optilab rEX) and fitted with a PLgel 5 μm mixed-D column calibrated using linear polystyrene standards. The thermal properties of the azo molecular glasses were investigated with a TA instrument (DSC 2910 and Hi-Res TGA 2950) at a heating rate of 10 °C min^{-1} under N_2 protection. The surface profiles of the surface-relief-gratings and self-structured surface patterns were monitored using an atomic force microscope (AFM, Nanoscope IIIa, tapping mode).

2.3 Film preparation

Solid films of the azo molecular glasses with smooth surfaces were prepared by spin-coating. The azo compounds were dissolved in anhydrous *N*,*N*-dimethylformamide (DMF) to obtain homogeneous solutions with concentrations about 15 wt%. The solutions were filtered through 0.45 μm membranes and spin-coated onto glass slides. The film thickness was controlled to be in a range from 200 nm to 400 nm by adjusting the spinning speed. The films were dried at 60–70 °C under vacuum for 48 h.

2.4 Laser irradiation

A linearly or circularly polarized beam from a diode-pumped frequency doubled solid state laser (532 nm) was used as the light source. The laser beam with an intensity of 200 mW cm^{-2} was obtained after being spatially filtered, expanded and collimated. For inducing the self-structured surface patterns, the laser beam was incident perpendicularly on the film surfaces.[30] SRG inscription was carried out by the experimental setup and conditions similar to those reported before.[9,10] A p-polarized beam from the diode-pumped frequency doubled solid state laser at 532 nm with an intensity of about 80 mW cm^{-2} was used as the writing beam. The writing beam was split by a mirror such that a half of the beam reflected onto the film surface was coincident with the other half of the beam to form an interference pattern. The formation of SRGs was probed with an unpolarized low power He–Ne laser beam at 633 nm by measuring the diffraction efficiency of the first-order diffracted beam in a real time mode.

3 Result and discussion

3.1 Synthesis and characterization

The synthetic route of the star-shaped molecules containing both azo chromophores and carbazole moieties is given in Scheme 1. The syntheses started from the preparation of two precursors **Tr-AN** and **6-Tr-AN** to obtain the core structures. The precursor **Tr-AN** was obtained by the ring open reaction of 1,3,5-triglycidyl isocyanurate (TGIC) with *N*-methylaniline (AN). The experimental details of this step have been reported in our recent publication.[30] **6-Tr-AN** was synthesized by a similar procedure but using *N*-(2-hydroxyethyl)aniline instead of *N*-methylaniline. The carbazole moieties were introduced by the esterification reaction between the 6-(*H*-carbazol-9-yl)hexanoic acid and the precursors. The reactions were catalyzed by 4-dimethylaminopyridine (DMAP) through a routine esterification procedure activated by dicyclohexyl-carbodiimide (DCC). The target molecules were finally obtained from the two kinds of carbazole-containing precursors by the azo-coupling reactions using diazonium salts of the two aniline derivatives. This reaction route could introduce azo chromophores with different electron-withdrawing groups at the final stage of the preparation under mild conditions. The diazonium salts readily attack

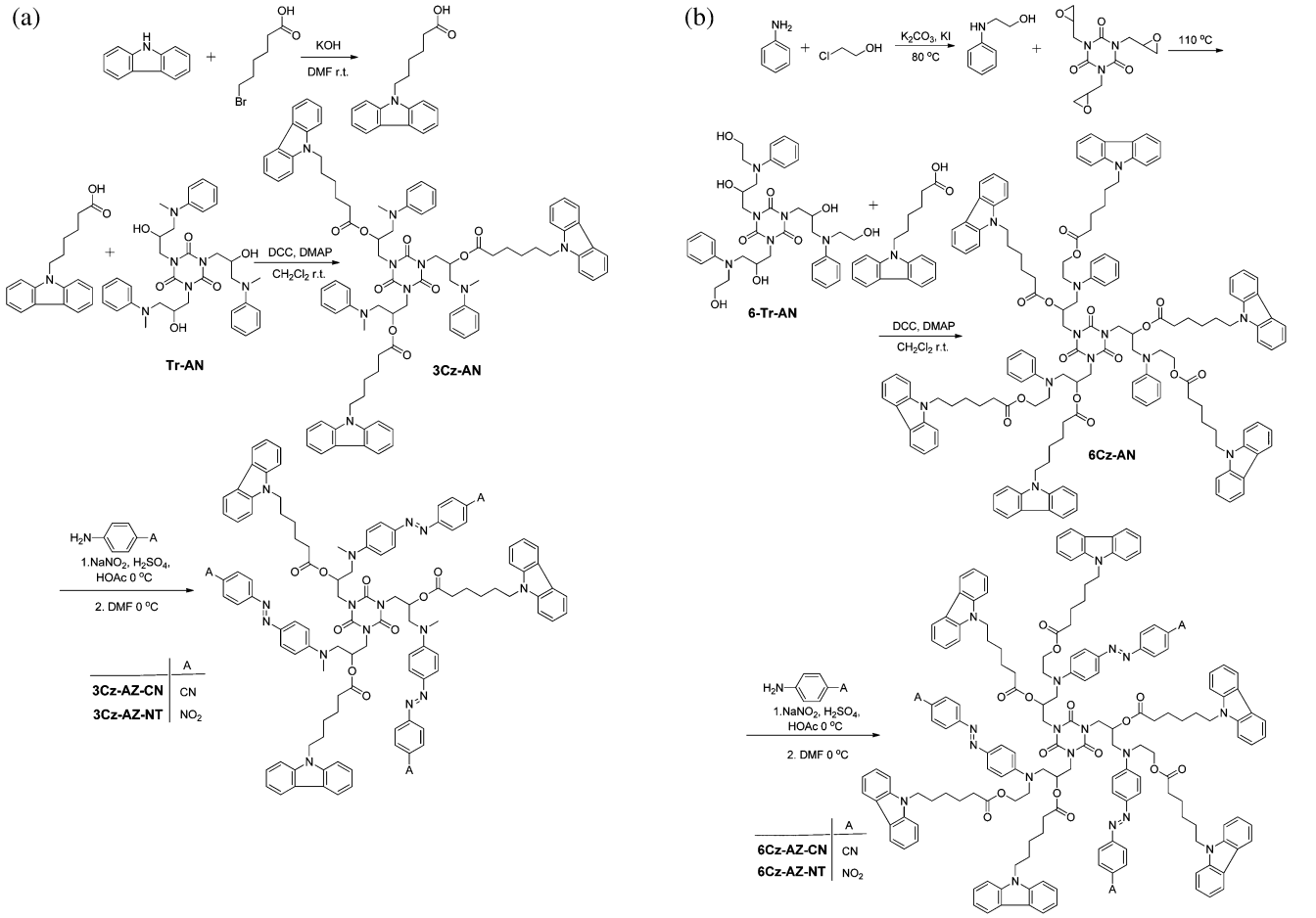

Scheme 1 (a) Synthetic route of the star-shaped molecules **3Cz-AZ-CN** and **3Cz-AZ-NT**. (b) Synthetic route of the star-shaped molecules **6Cz-AZ-CN** and **6Cz-AZ-NT**.

the benzene rings of the anilino groups at positions with high electron densities. The bulkiness of the attacking groups and the resulting steric hindrance allow the electrophilic substitution to take place exclusively at the *para* position. This synthetic route can be used to prepare a series of star-shaped molecules bearing different electron-withdrawing groups. The chemical structure of the star-shaped molecules was confirmed by spectroscopic analyses as shown by the data given in the Experimental section.

3.2 Thermal and spectral properties

The thermal transition and phase behavior of the star-shaped molecules were investigated by differential scanning calorimetry (DSC) and polarized optical microscopy (POM). The DSC curves of the four azo compounds given in Fig. 1 show the typical glass transition behavior. The glass transition temperatures (T_gs) obtained from DSC are summarized in Table 1. The T_gs of the **3Cz-AZ-CN**, **3CZ-AZ-NT**, **6Cz-AZ-CN** and **6Cz-AZ-NT** are 89, 86, 74 and 73 °C, respectively. The **6Cz-AZ-X** (X = CN and NT) molecules have relatively lower T_gs, which could be attributed to more carbazole moieties in the molecules. POM observations indicated that before and after the glass transition, all samples of **3Cz-AZ-X** and **6Cz-AZ-X** (X = CN and NT) were isotropic and did not show optical birefringence caused by preferential molecular orientation. Thermogravimetric analysis (TGA) was used to investigate the thermal stability of the azo compounds. TGA curves of the azo compounds are shown in Fig. 2 and the thermal decomposition temperatures (T_ds) obtained from TGA are summarized in Table 1. The T_ds of **3Cz-AZ-CN**, **3CZ-AZ-NT**,

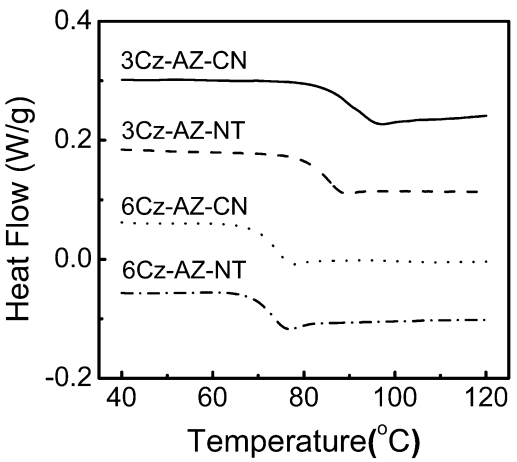

Fig. 1 DSC curves of the azo molecular glasses.

Table 1 T_gs, T_ds and λ_{max}s of **3Cz-AZ-CN**, **3CZ-AZ-NT**, **6Cz-AZ-CN** and **6Cz-AZ-NT**

Sample	T_g (°C)	T_d (°C)	λ_{max} (nm)[a]
3Cz-AZ-CN	89	279	445
3Cz-AZ-NT	86	312	458
6Cz-AZ-CN	74	322	443
6Cz-AZ-NT	73	325	469

[a] In DMF solution.

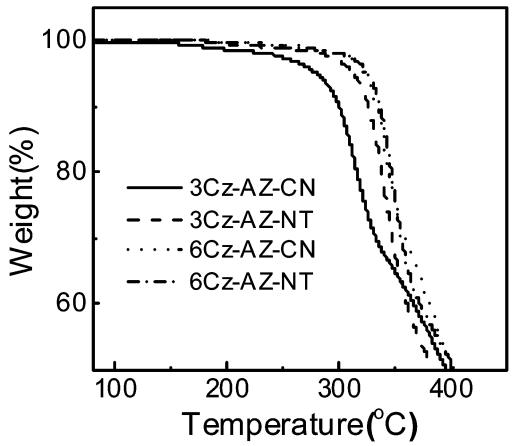

Fig. 2 TGA curves of the star-shaped molecules.

6Cz-AZ-CN and **6Cz-AZ-NT** are 279, 312, 322 and 325 °C, respectively.

The UV-vis spectra of the azo compounds in DMF solutions are given in Fig. 3. The spectra show typical characteristics of a pseudo-stilbene-type azo compound.[2] The absorption bands corresponding to the π–π* transition appear in the visible spectral region and the azo compounds exhibit a bright colour owing to the strong absorption. The weak n–π* transition band overlaps with the π–π* transition band and cannot be seen separately. The positions of the π–π* transition bands are strongly affected by the electron-withdrawing groups on the azobenzene moieties, which can be attributed to their inductive and conjugative effects on both the ground and excited states. On the other hand, the band positions are also related to the molecular structure, such as those observed for **3CZ-AZ-NT** and **6Cz-AZ-NT**. The λ_{max}s of **3Cz-AZ-CN**, **3CZ-AZ-NT**, **6Cz-AZ-CN** and **6Cz-AZ-NT** are 445, 458, 443 and 469 nm (Table 1).

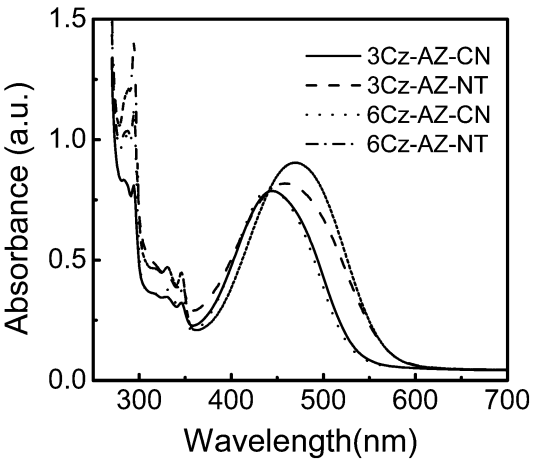

Fig. 3 UV-vis spectra of the star-shaped molecules in DMF solutions.

3.3 Photoinduced self-structured pattern formation

To compare the photoresponsive properties of the azo compounds, the self-structured surface pattern formation on **3Cz-AZ-CN**, **3CZ-AZ-NT**, **6Cz-AZ-CN** and **6Cz-AZ-NT** films was studied. The solid films of the azo molecular glasses were irradiated with a uniform laser beam (532 nm, 200 mW cm^{-2}) at the normal incidence. Fig. 4 shows the typical AFM images of the photoinduced surface patterns on the **3Cz-AZ-X** (X = CN and NT) films after irradiating for 30 min. The surface patterns comprise regularly spaced structures. Some localized arrangement of the surface structures can be recognized from the images. With the same irradiation time and light intensity, obvious differences in their morphology can be seen for the surface patterns induced by irradiation with linearly or circularly polarized laser lights.

For **3Cz-AZ-CN**, when irradiated with linearly polarized light, the surfaces show partially merged pillar-like structures with some localized hexagonal arrangement (Fig. 4(a)). The alignment of the hexagonal patterns shows some correlation with the polarization direction of the laser beam. The period of the regularly spaced pillars is 540 ± 10 nm, which is estimated along ±60 degrees with respect to the light polarization direction. The amplitude of the surface modulation is about 60 nm. When irradiated with circularly polarized light, no such localized hexagonal patterns can be seen (Fig. 4(b)). The surface

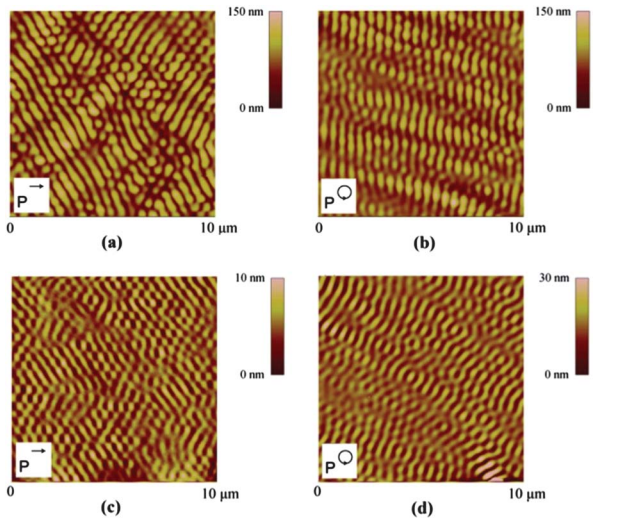

Fig. 4 Typical AFM images (10 μm × 10 μm) of the photoinduced self-structured surface patterns on **3Cz-AZ-X** films induced by light with the different polarizations: (a) **3Cz-AZ-CN**, linearly polarized; (b) **3Cz-AZ-CN**, circularly polarized; (c) **3Cz-AZ-NT**, linearly polarized and (d) **3Cz-AZ-NT**, circularly polarized. The intensity of the laser beam was 200 mW cm^{-2} and the irradiation time was 30 min.

patterns appear like ripple stripes with some periodicity between them. The amplitude of the surface modulation induced by the circularly polarized light is about 80 nm.

For **3Cz-AZ-NT**, when irradiated with light under the same conditions, the amplitude of the surface modulation is much smaller compared to **3Cz-AZ-CN**. After being irradiated with linearly polarized light, the heights of pillars on **3Cz-AZ-NT** films are only about 7 nm, which shows the period of 510 ± 10 nm. For the sample irradiated with a circularly polarized laser beam, the amplitude is about 15 nm. Similar to **3Cz-AZ-CN**, the morphology also shows a close reliance on the light polarization condition (Fig. 4(c) and (d)).

Fig. 5 shows the typical AFM images of the surface morphology on the **6Cz-AZ-X** (X = CN and NT) films after irradiating for 30 min. Among these two compounds, only **6Cz-AZ-CN** shows weak ability to form the self-structured pattern with the pillar height about 7 nm, when irradiated with circularly polarized light. For **6Cz-AZ-CN** irradiated with linearly polarized light and **6Cz-AZ-NT** irradiated with both linearly and circularly polarized light, only irregular surface roughness can be seen after the light irradiation.

The above observation clearly indicates the correlation of pattern formation with the azo chromophore. The photoinduced pattern formation behavior of the star-shaped molecules is obviously different for these two kinds of azo chromophores, which show difference only in the electron-withdrawing groups. The two molecules bearing the cyano-substituted azo chromophore show the higher efficiency to form the self-structured surface pattern. On the other hand, the chromophore density also plays an important role in the formation of these regular surface patterns. A high enough chromophore density is necessary for the self-structured pattern formation. This point is consistent with our previous reports about photoinduced self-structured pattern formation for linear azo polymers.[34]

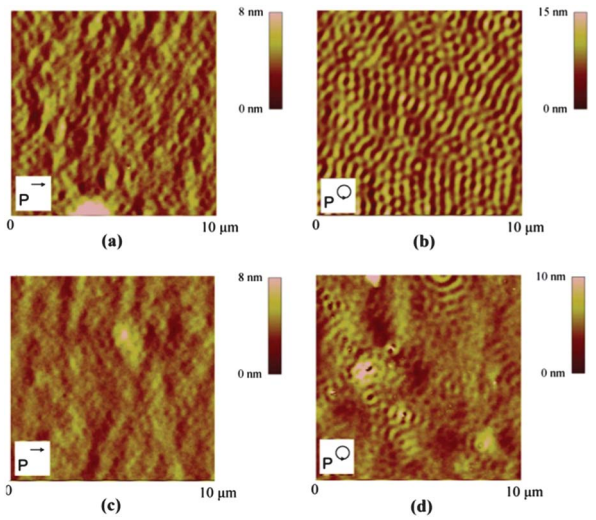

Fig. 5 Typical AFM images (10 μm × 10 μm) of the photoinduced self-structured surface patterns on **6Cz-AZ-X** films induced by light with the different polarizations: (a) **6Cz-AZ-CN**, linearly polarized; (b) **6Cz-AZ-CN**, circularly polarized; (c) **6Cz-AZ-NT**, linearly polarized and (d) **6Cz-AZ-NT**, circularly polarized. The intensity of the laser beam was 200 mW cm^{-2} and the irradiation time was 30 min.

3.4 Photoinduced surface-relief-gratings

Photoinduced SRG formation on *n*Cz-AZ-X (*n* = 3 or 6, X = CN or NT) films was investigated by using interfering p-polarized laser beams (532 nm, 80 mW cm^{-2}) as the inscribing light and a He–Ne laser beam at 633 nm as the probe beam. The SRG formation was monitored by measuring the first-order diffraction efficiencies of the probe beam in a real-time manner. The profiles and trough depths of the gratings were detected by AFM. Upon exposure to the interference pattern of laser beams at the modest intensity, SRGs were formed on films of all four azo molecular glasses. Fig. 6 shows a typical AFM image of the sinusoidal surface relief structures with regular spaces formed on the **6Cz-AZ-NT** films. The spatial period depends on the wavelength and the incident angle of the writing beams. Like those reported for azo polymer films, the SRGs are stable below the T_gs of the amorphous materials and can be removed by heating the samples to a temperature above their T_gs.

For a comparative study, films of the four azo molecular glasses were exposed to laser light when the experimental conditions, such as the laser intensity, incident angle and film thickness, were controlled to be identical. Fig. 7 shows the first-order diffraction efficiency (DE) as a function of irradiation time for *n*Cz-AZ-X (*n* = 3 or 6, X = CN or NT). The result shows that the SRG-forming rate is closely related to structures of the molecular glasses and the electron-withdrawing groups of the azo chromophores.

Molecules containing the cyano-substituted azo chromophores, **3Cz-AZ-CN**, shows a faster growth rate during the SRG formation than **6Cz-AZ-CN** owing to the higher azo chromophore density of the former. However, an opposite tendency is observed for the molecules containing the nitro-substituted azo chromophores. **3Cz-AZ-NT** shows a slower SRG-growth rate than that of **6Cz-AZ-NT**. An important point can be seen by comparing the difference between the molecules with the same azo density but bearing the cyano- or nitro-substituted chromophores. For **3Cz-AZ-X** (X = CN or NT), **3Cz-AZ-CN** forms SRG much faster than **3Cz-AZ-NT** does, which is coincident with most of the previous reports for azo molecular glasses and azo polymers.[28,29,35,36] However, the SRG growth rate of **6Cz-AZ-NT** is extraordinarily high, which is almost the same as that of **3Cz-AZ-CN** and much higher than that of **6Cz-AZ-CN**. This

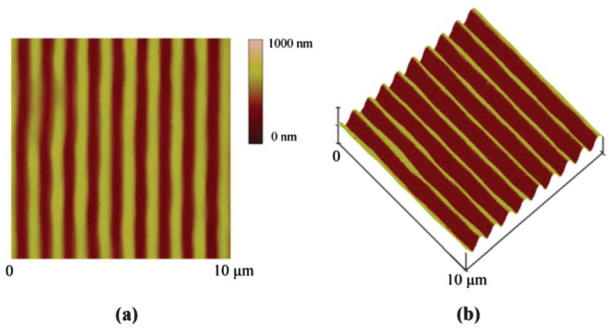

Fig. 6 AFM images of the surface-relief-gratings on the **6Cz-AZ-NT** film, (a) 2D view and (b) 3D view. The intensity of the laser beam was 80 mW cm^{-2} and the irradiation time was 600 s.

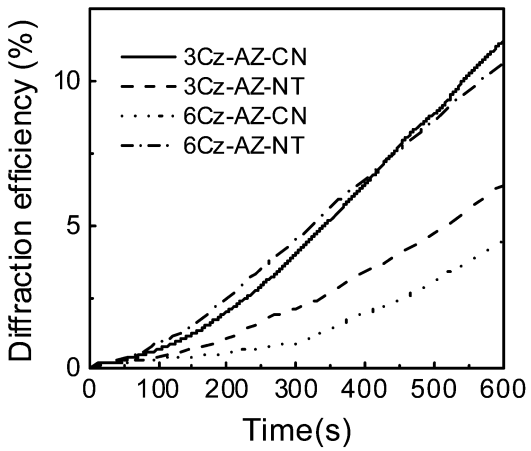

Fig. 7 Diffraction efficiency as a function of the irradiation time for **3Cz-AZ-CN**, **3CZ-AZ-NT**, **6Cz-AZ-CN** and **6Cz-AZ-NT**.

observation indicates that the slower SRG growth rate observed for the materials containing nitro-substituted azo chromophores could be attributed to the strong dipole–dipole interaction between the azo chromophores. For **6Cz-AZ-NT**, the low chromophore density and the branched structure help to separate the azo chromophores and can avoid the dipole–dipole interaction and result in a high SRG growth rate.

3.5 Discussion

The above investigation on the photoinduced formation of self-structured surface patterns and SRGs can shed some new light on how to further improve the molecular design. It is generally agreed that the mass-transfer behavior is caused by or directly related to the *trans–cis* isomerization of azo chromophores.[11–18] Therefore, this effect should be enhanced by increasing the chromophore density. On the other hand, the strong dipole–dipole interaction between the chromophores could restrain the chain motion in some cases. As indicated by previous studies, SRG can be inscribed on films of polymers with a relatively low chromophore density.[34,35] Therefore, some buffer groups can be introduced into the molecular structures to separate the azo chromophores to avoid strong dipole–dipole interaction as demonstrated above using **6Cz-AZ-NT**. On the other hand, as the self-structured surface pattern formation requires a high azo chromophore density,[34] azo chromophores with low dipole moment such as the cyano-substituted one are more suitable for this application.

Carbazole is well known as a functional group for many applications. Poly(*N*-vinylcarbazole) (PVK) has been used as a photoconductive polymer in photocopiers for years.[32] The molecules prepared in this study could be investigated for other functionalities. As the molecules contain both carbazole units and azo chromophores, they can possibly be used as photorefractive materials by exploiting their space-charge-field formation and electro-optic nonlinearity.[31,37] Moreover, if the photoactive properties of the carbazole units have some influence on the mass-transfer properties reported above also needs further investigation.

4 Conclusions

A new class of star-shaped molecules, containing both azo chromophores and carbazole groups (*n*Cz-AZ-X, $n = 3$ or 6, X = CN or NT), was synthesized in this work. The materials show the behavior of an amorphous solid at room temperature requiring no special treatments such as quenching. The type of azo chromophore, the number of the carbazole groups and the molecular architecture all play important roles to influence both the photoinduced self-structured surface pattern formation and SRG inscription rate. The molecular design using the flexible spacer to incorporate the carbazole groups can significantly enhance the SRG formation efficiency of the materials containing the nitro-substituted azo chromophores. This understanding can be further explored for developing materials with better performance. The materials could be potentially used for other applications by further exploring the functions of carbazole groups.

Acknowledgements

The financial support from NSFC under Projects 51233002 and 91027024 is gratefully acknowledged.

Notes and references

1 G. S. Kumar and D. C. Neckers, *Chem. Rev.*, 1989, **89**, 1915–1925.
2 H. Rau, in *Photochemistry and Photophysics*, ed. J. F. Rabek, CRC Press, Boca Raton FL, 1990, vol. 2, ch. 4.
3 A. Natansohn, P. Rochon, J. Grosselin and S. Xie, *Macromolecules*, 1992, **25**, 2268–2273.
4 S. Xie, A. Natansohn and P. Rochon, *Chem. Mater.*, 1993, **5**, 403–411.
5 J. A. Delaire and K. Nakatani, *Chem. Rev.*, 2000, **100**, 1817–1845.
6 A. Natansohn and P. Rochon, *Chem. Rev.*, 2002, **102**, 4139–4175.
7 N. K. Viswanathan, D. Y. Kim, S. P. Bian, J. Williams, W. Liu, L. Li, L. Samuelson, J. Kumar and S. K. Tripathy, *J. Mater. Chem.*, 1999, **9**, 1941–1955.
8 (*a*) T. Ikeda, J. Mamiya and Y. Yu, *Angew. Chem., Int. Ed.*, 2007, **46**, 506–528; (*b*) A. Shishido, *Polym. J.*, 2010, **42**, 525–533; (*c*) H. F. Yu and T. Ikeda, *Adv. Mater.*, 2011, **23**, 2149–2180; (*d*) T. Yoshino, M. Kondo, J. I. Mamiya, M. Kinoshita, Y. L. Yu and T. Ikeda, *Adv. Mater.*, 2010, **22**, 1361–1363.
9 P. Rochon, E. Batalla and A. Natansohn, *Appl. Phys. Lett.*, 1995, **66**, 136–138.
10 D. Y. Kim, S. K. Tripathy, L. Li and J. Kumar, *Appl. Phys. Lett.*, 1995, **66**, 1166–1168.
11 (*a*) C. J. Barrett, A. L. Natansohn and P. L. Rochon, *J. Phys. Chem.*, 1996, **100**, 8836–8842; (*b*) C. J. Barrett, P. Rochon and A. Natansohn, *J. Chem. Phys.*, 1998, **109**, 1505–1516.
12 (*a*) J. Kumar, L. Li, X. L. Jiang, D. Y. Kim, T. S. Lee and S. Tripathy, *Appl. Phys. Lett.*, 1998, **72**, 2096–2098; (*b*) S. Bian, J. Williams, D. Kim, L. Li, S. Balasubramanian, J. Kumar and S. Tripathy, *J. Appl. Phys.*, 1999, **86**, 4498–4508.

13 T. G. Pedersen, P. M. Johansen, N. C. R. Holme and P. S. Ramanujam, *Phys. Rev. Lett.*, 1998, **80**, 89–92.
14 P. Lefin, C. Fiorini and J. Nunzi, *Pure Appl. Opt.*, 1998, **7**, 71–82.
15 O. M. Tanchak and C. J. Barrett, *Macromolecules*, 2005, **38**, 10566–10570.
16 (*a*) K. G. Yager, O. M. Tanchak, C. Godbout, H. Fritzsche and C. J. Barrett, *Macromolecules*, 2006, **39**, 9311–9319; (*b*) K. G. Yager and C. J. Barrett, *Macromolecules*, 2006, **39**, 9320–9326.
17 C. Hubert, C. Fiorini-Debuisschert, I. Maurin, J. M. Nunzi and P. Raimond, *Adv. Mater.*, 2002, **14**, 729–732.
18 C. Hubert, C. Fiorini-Debuisschert, L. Rocha, P. Raimond and J. Nunzi, *J. Opt. Soc. Am. B*, 2007, **24**, 1839–1846.
19 (*a*) Y. Shirota, *J. Mater. Chem.*, 2000, **10**, 1–25; (*b*) Y. Shirota, *J. Mater. Chem.*, 2005, **15**, 75–93.
20 E. Ishow, C. Bellaïche, L. Bouteiller, K. Nakatani and J. A. Delaire, *J. Am. Chem. Soc.*, 2003, **125**, 15744–15745.
21 Y. Shirota, K. Moriwaki, S. Yoshikawa, T. Ujike and H. Nakano, *J. Mater. Chem.*, 1998, **8**, 2579–2581.
22 (*a*) A. Perschke and T. Fuhrmann, *Adv. Mater.*, 2002, **14**, 841–843; (*b*) T. Fuhrmann and T. Tsutsui, *Chem. Mater.*, 1999, **11**, 2226–2232.
23 (*a*) C. Chun, M. Kim, D. Vak and D. Kim, *J. Mater. Chem.*, 2003, **13**, 2904–2909; (*b*) M. Kim, E. Seo, D. Vak and D. Kim, *Chem. Mater.*, 2003, **15**, 4021–4027.
24 (*a*) H. Utsumi, D. Nagahama, H. Nakano and Y. Shirota, *J. Mater. Chem.*, 2000, **10**, 2436–2438; (*b*) H. Utsumi, D. Nagahama, H. Nakano and Y. Shirota, *J. Mater. Chem.*, 2002, **12**, 2612–2619.
25 (*a*) H. Ando, T. Tanino, H. Nakano and Y. Shirota, *Mater. Chem. Phys.*, 2009, **113**, 376–381; (*b*) H. Nakano, T. Takahashi, T. Kadota and Y. Shirota, *Adv. Mater.*, 2002, **14**, 1157–1160; (*c*) H. Nakano, T. Tanino, T. Takahashi, H. Ando and Y. Shirota, *J. Mater. Chem.*, 2008, **18**, 242–246; (*d*) T. Tanino, S. Yoshikawa, T. Ujike, D. Nagahama, K. Moriwaki, T. Takahashi, Y. Kotani, H. Nakano and Y. Shirota, *J. Mater. Chem.*, 2007, **17**, 4953–4963.
26 E. Ishow, B. Lebon, Y. N. He, X. G. Wang, L. Bouteiller, L. Galmiche and K. Nakatani, *Chem. Mater.*, 2006, **18**, 1261–1267.
27 A. S. Matharu, S. Jeeva, P. R. Huddleston and P. S. Ramanujam, *J. Mater. Chem.*, 2007, **17**, 4477–4482.
28 Y. N. He, X. Y. Gu, M. C. Guo and X. G. Wang, *Opt. Mater.*, 2008, **31**, 18–27.
29 G. Ye, D. R. Wang, Y. N. He and X. G. Wang, *J. Mater. Chem.*, 2010, **20**, 10680–10687.
30 J. J. Yin, G. Ye and X. G. Wang, *Langmuir*, 2010, **26**, 6755–6761.
31 M. J. Cho, D. H. Choi, P. A. Sullivan, A. J. P. Akelaitis and L. R. Dalton, *Prog. Polym. Sci.*, 2008, **33**, 1013–1058.
32 P. L. T. Boudreault, S. Beaupré and M. Leclerc, *Polym. Chem.*, 2010, **1**, 127–136.
33 J. Li and A. C. Grimsdale, *Chem. Soc. Rev.*, 2010, **39**, 2399–2410.
34 X. L. Wang, J. J. Yin and X. G. Wang, *Macromolecules*, 2011, **44**, 6856–6867.
35 Y. N. He, X. G. Wang and Q. X. Zhou, *Polymer*, 2002, **43**, 7325–7333.
36 Y. N. He, X. G. Wang and Q. X. Zhou, *Synth. Met.*, 2003, **132**, 245–248.
37 O. Ostroverkhova and W. E. Moerner, *Chem. Rev.*, 2004, **104**, 3267–3314.

